13

Application of Carbon Nanotubes to Mirror Actuators for Space Laser Communications

Yoshihisa Takayama and Morio Toyoshima
National Institute of Information and Communications Technology
Japan

1. Introduction

Recently free-space laser communications attract attentions as one of the promising technologies to provide broadband wireless communications. Especially in the inter-satellite communications and the satellite-ground communications, the successful demonstrations showed the possibilities of the laser communications for the practical use (Tolker-Nielsen, 2002; Jono, 2006; Smutny, 2008; Toyoshima, 2009; Perlot, 2007).

Concerning the laser communication equipment used in those demonstrations, the designs are mutually different but some functions are commonly used. The typical example is a function to control the direction of the telescope. Some terminals have a motorized gimbals system to hold a telescope and control the direction of the aperture. The other terminals use a set of mirrors put in front of a fixed telescope aperture, and the direction of the telescope view is changed by using the reflection of the mirrors. These direction steering functions are usually employed for the coarse pointing of a communicating object. In the internal optics of the communication equipment, two sets of moving mirrors are found in most cases. One is a set of fast steering mirrors for the fine pointing mechanisms and the other is a similar set of mirrors to give a point-ahead angle to the emitted laser beam. Since the laser communications require accurate pointing for stable communications, the fine pointing mechanisms are necessary to eliminate the angular errors remained after the coarse tracking by the telescope. Besides, when the laser communications are carried out between moving objects, the fast velocities of satellites and the large distance between communicating terminals require the point-ahead angles (Miller, 1993). So far, in those kinds of functions, the tilt angle of the mirrors is controlled by piezoelectric actuators, voice coils, micro-electro-mechanical systems, diaphragms with electromagnetic torque, spherical motors, and so on (Aoki, 2004; Suhonen, 2001; Bandera, 1999; Langenbach, 2005).

When equipment is mounted in a satellite, we should care that the resources such as the mass, the volume and the consumption power for the equipment are severely restricted. Therefore, devices of light weight, small size and low power consumption are useful for constructing those tracking and pointing mechanisms.

On the other hand, in the field of electro-active polymer actuators, many research activities have been reported to develop materials responding to applied stimuli such as temperature, magnetism and electricity (Baughman, 1999; Jordan, 2007; Lu, 2008). Those materials are aimed to be utilized in biomimetic motions, micro-electro-mechanical-systems, sensors, and precise positioners. The features of the polymer actuators are the low voltage operations, light weight,

large stretching characteristics and mechanically simple structure which conform to the requirements for constructing small, light and low power consumption laser communications equipment. Furthermore the flexibility in the shape design implies the applicability of the actuator in various manners. Therefore, we look at the possibilities of the actuators to be applied to the moving parts in the laser communication terminals (Takayama, 2010).
The polymer actuators require wet for operation because the fundamental is swell due to ionic mobility. Therefore if the actuators are used in the steering mirror functions, especially in space environment, an approach to prevent the evaporation of moisture becomes necessary. As the solution to suppress the evaporation of moisture, the use of the ionic liquid is one of the effective approaches.
In this chapter, we would like to study a potential of the polymer actuators to be used in the optical terminals. First, we show a typical example of a laser communication terminal and introduce the functions that consist of mechanical steering parts. Second, we perform numerical analyses to study the operation requirements on those parts. For the study, a scenario in which an optical ground station and a satellite in a low earth orbit carry out laser communications is assumed. The angular operations of the movable parts to track the communicating counter object are estimated. As the third step, we fabricate a prototype of a carbon nanotube actuator that is employed as a steering function of the reflection angle of a mirror. By using this sample, the angular operation characteristics of the actuator are investigated. Here we employ a perfluorosulfonic acid ionomer, an imidazole tetrafluoroborate for the fabrication processes as the ionic liquid and carbon single-walled nanotube covered with a gold layer for the electrode. With changing the applied voltage to the actuator, the mirror's reflection angle is measured.

2. Space laser communication terminal and requirements on actuators operation characteristics

In this section, we provide a sample structure of a laser communication terminal in order to identify the movable parts discussed here. These are the intended potential targets to be replaced with the carbon actuators. The roles of the steering functions are introduced respectively and the required angular operations of those movable parts are calculated with assuming a scenario in which the optical ground station and a satellite perform the laser communications.

2.1 Optical communication terminal

An example of optical terminals for space laser communications is shown in the figure 1, where the solid bold lines indicate the propagating paths of the received beam and the dashed bold lines show the path of the transmitted beam. In most cases, three mechanically movable parts, the coarse pointing function, the fine pointing function and the point-ahead function, are contained.
The coarse pointing function controls the pointing direction of the telescope to keep looking at the communicating object. If the object moves, the telescope tracks the object. The optical characteristics are dependent on the design of the communication system. But as an example of a terminal successfully operated in space, we have that the field-of-view of the telescope is ±0.2deg and the tracking accuracy is within ±0.01deg (Jono, 2006).
Even if the coarse pointing function controls the direction of the telescope aperture precisely, the arrival angle of the received beam still changes within the tracking accuracy of

the coarse pointing function. Therefore the fine pointing function is employed to eliminate such small but rapid angular changes remaining in the received beam. The continuous elimination of the angular uncertainty in the arrival beam is equivalent to instantaneously find the precise direction of the communicating counter object as well as providing the stable illumination of the optical receiver to detect the signal.
When the communicating object moves fast, angular compensation is required in the pointing direction of the beam transmission. The difference between the arrival angle of the received beam and the pointing direction of the transmission beam is observed when the travel distance of the counter object cannot be ignored during the period of the propagation of light. The point-ahead function gives the compensation angle to the propagation direction of the transmitted light.
These three functions have their own optical sensors as shown in the figure 1. The coarse pointing and the fine pointing functions use the sensors to detect the received light for the closed-loop steering, while the sensor of the point-ahead function detects the transmitted light.

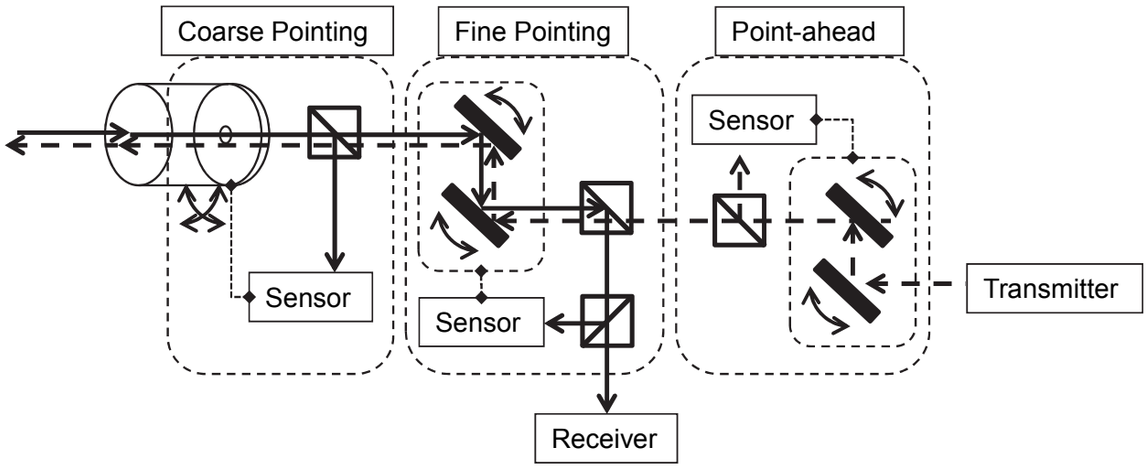

Fig. 1. Schematic drawing of an optical communication terminal. The solid bold lines indicate the optical path of the received beam and the dashed bold lines are the path of the transmitted beam.

2.2 Requirement in angular movement for coarse pointing

To estimate the angular range of the moving parts in the optical terminal, we focus on the satellite-ground laser communications. Here we assume to track the International Space Station (ISS) as the one of the widely recognized satellites by using an optical ground station. The ISS orbits the earth at an altitude of about 400 km which is regarded as a low earth orbit.
The direction of the communicating counter object can be described by the pair of angles of the azimuth and the elevation. In the case of the ground stations, the basis to measure these angles is the horizontal plane and the zenith at the ground station. But in the case of the satellite, the basis depends on the satellite attitude. Since the satellite attitude changes with orbiting the earth, we concentrate on the azimuth angle and the elevation angle at a ground station in the following analysis for the sake of simplicity.
The date of the orbit computation is assumed as 2nd Oct. 2010, for instance. The azimuth angle and the elevation angle measured at the ground stations to track the ISS are shown in

the figures 2(a) and 2(b), respectively. In these figures, the curves labelled with (1) are the calculation results for the optical ground station located in Tokyo, Japan. The latitude and the longitude are given as 35.7deg and 139.5deg, respectively. For the labels of (2)-(5), we keep the latitude of the ground station as the same as 35.7deg but change the longitude as 149.5deg, 159.deg, 169.5deg, and 219.5deg, respectively, in order to obtain the different maximum elevation angles. The corresponding maximum elevation angles are obtained as 34.3deg, 64.2deg, 88.6deg, 87.9deg and 56.3deg for (1)-(5).

The figure 3(a) and 3(b) are the absolute values of the azimuth angle rate and the elevation angle rate obtained from the figures 2(a) and 2(b). Concerning the angular rates for the azimuth and the elevation angles, faster motion is required in the azimuth for the case of high elevation angles. Theoretically the rotation velocity around the azimuth axis is required to be infinite if the ground station tracks the object passing right above the zenith of the ground station.

According to those calculations shown in the figures 2 and 3, the requirement in angular movement is that the angular range of the azimuth should be more than 360deg, and the range of the elevation is from 0 to 90deg. The rate of the angular motion is more than 48deg/s for the azimuth if we intend to track a satellite passing almost right above the ground station, while the rate is less than 1.2deg/s for the elevation.

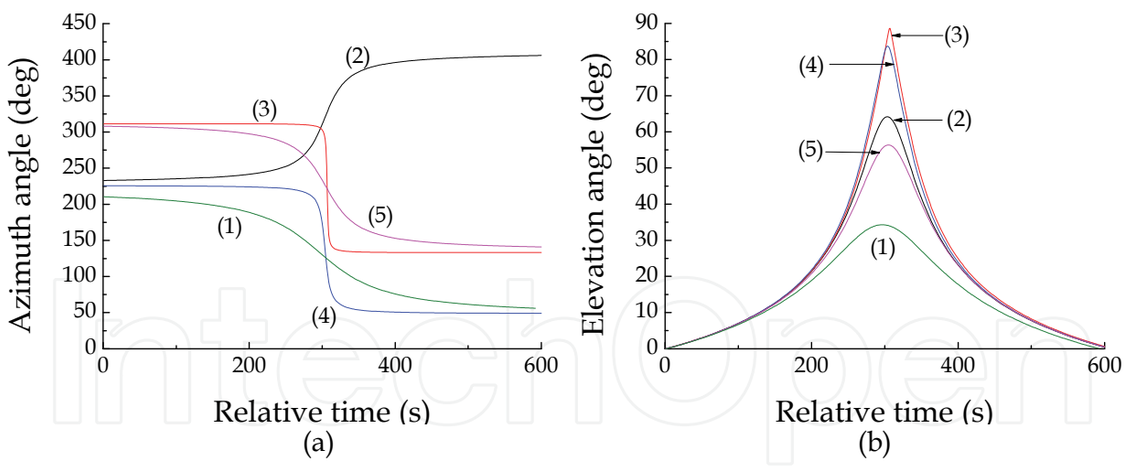

Fig. 2. (a) Azimuth angle and (b) elevation angle at ground station to track the ISS. The labels (1)-(5) indicate the observation points. The longitude is 139.5deg for the label (1), 149.5deg for (2), 159.5deg for (3), 169.5deg for (4) and 219.5deg for (5). The location's latitude is fixed as 35.7deg.

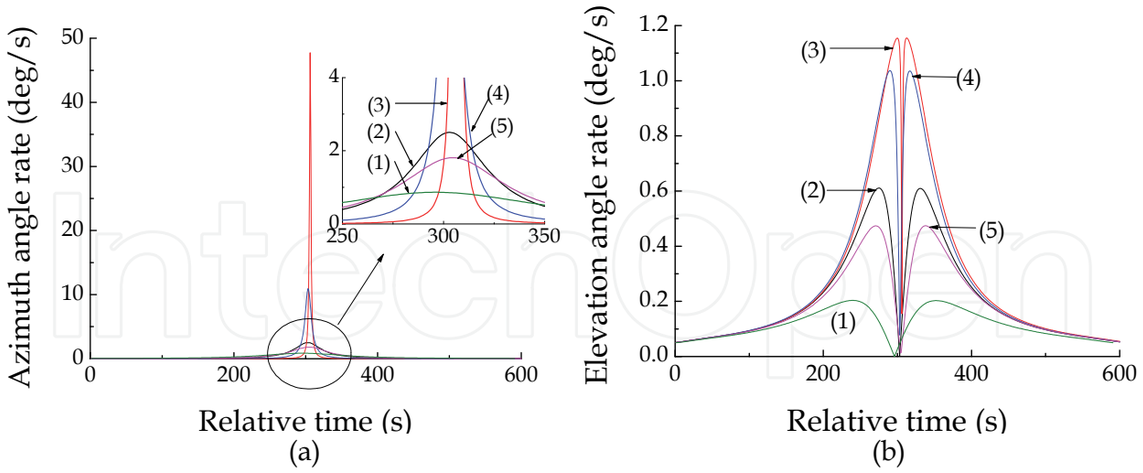

Fig. 3. Absolute values of (a) azimuth angle rate and (b) elevation angle rate to track the ISS.

2.3 Requirement in angular movement for fine pointing and point-ahead functions

The coarse pointing function steers the telescope to track the communicating object and the fine pointing function compensates the remaining propagation angle of the received beam inside the optical terminal as shown in the figure 1. In most cases, the propagation angle of the received beam led to the internal optics is magnified by a certain times. If the tracking accuracy of the coarse pointing function is given as ±0.01deg (Jono, 2006), and if he magnification is 10 times for example, the propagation angle range of the received beam in the internal optics extends to ±0.1deg. This could be regarded as the angular coverage for the fine pointing function.

The required point-ahead angle is dependent on the tangential component of the moving speed of the object. The orbiting velocity of the satellite v_{sat} is given as a function of the altitude as

$$v_{sat} = sqrt\left(g_c \,/\, \left(r_e + h_{sat}\right)\right) \tag{1}$$

, where g_c is the gravitational constant times mass of Earth, r_e is the radius of the earth, and h_{sat} is the altitude of a satellite (Miller, 1993). We set that g_c=398600.5km^3/s^2 and r_e=6378.14km and plot the velocity in the figure 4, where the abscissa axis is the altitude of a satellite. In this figure, the velocity is given as the left-hand ordinate axis. The velocity of a satellite is about 3km/s at the altitude of 36000km, and about 7.7km/s at the altitude of 400km.

The point-ahead angle θ_{PA} is given as

$$\theta_{PA} = 2v_{\tan} / c \tag{2}$$

, where v_{tan} is the tangential component of the object velocity and c is the velocity of the light (Miller, 1993). If we assume that the ground station locates in the orbit plane of a satellite and tracks the satellite passing through the zenith of the station, v_{tan} in the equation (2) becomes equivalent to v_{sat} in the equation (1). In this case, the point-ahead angle is proportional to the velocity. Therefore, the computed result is shown in the figure 4 with the right-hand ordinate axis. According to the result, the point-ahead angle is obtained as about 51μrad for the satellite at the altitude of 400km, and about 20μrad for the altitude of 36000km.

When the satellite is in a geostationary orbit, the elevation angle looking at it from the ground station is unchanged. But if the satellite is in a low earth orbit, the elevation angle at the ground station changes to track the satellite. Since the tangential component of a satellite depend on the elevation angle at the ground station, we calculate the point-ahead angle as a function of the elevation angle. The result is shown in the figure 5, where the altitude of a satellite is assumed as 400km, for instance. Besides, the angle rate for the point-ahead is shown in figure 6 as the same case as the label (3) in the figures 2 and 3. As a result, it is found that the angle rate could be less than 0.37μrad.

In the end of this section, it should be noted that among the three steering functions of the coarse pointing, the fine pointing and the point-ahead, only the fine pointing function needs the repeated back and forth motion, because the role of the fine pointing function is the compensation of the angular errors. On the other hand, the control manners of the coarse pointing function and the point-ahead function are monotonically increasing or decreasing as shown in the figures 2 and 5.

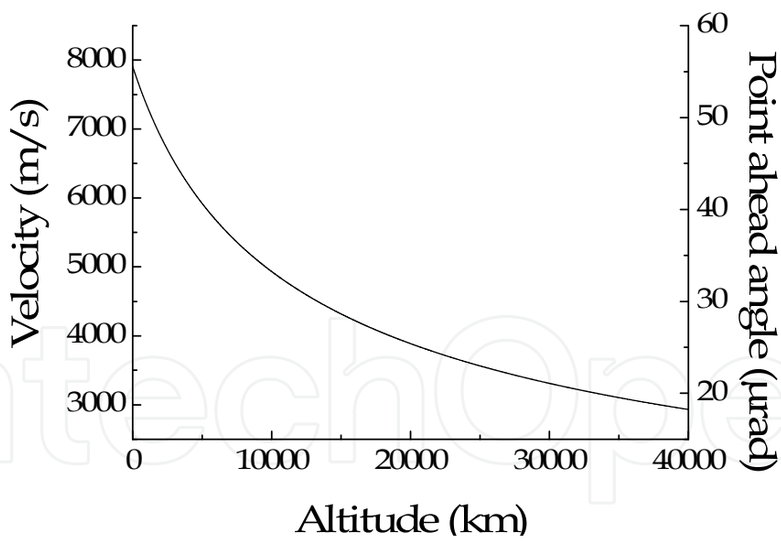

Fig. 4. Velocity of satellite as a function of the orbit altitude (the left-hand ordinate) and the point-ahead angle (the right-hand ordinate) in the case that the satellite passes through the zenith of the ground station.

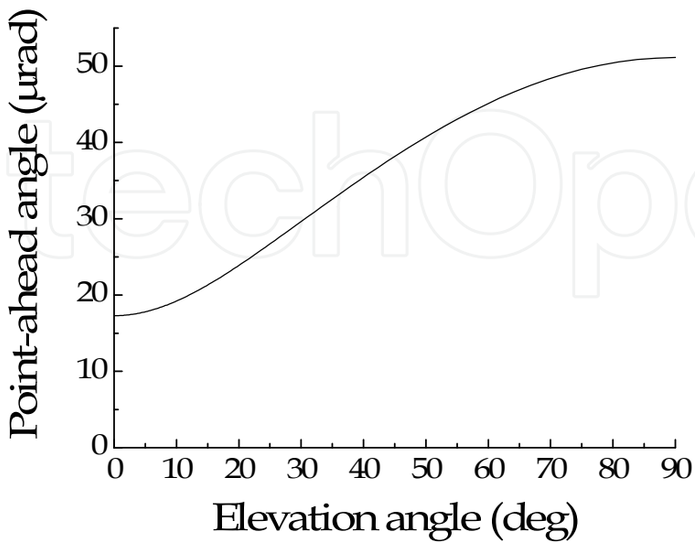

Fig. 5. Point-ahead angle as a function of the elevation angle at the ground station. The altitude of the satellite to be tracked is in a low earth orbit at the altitude of 400km.

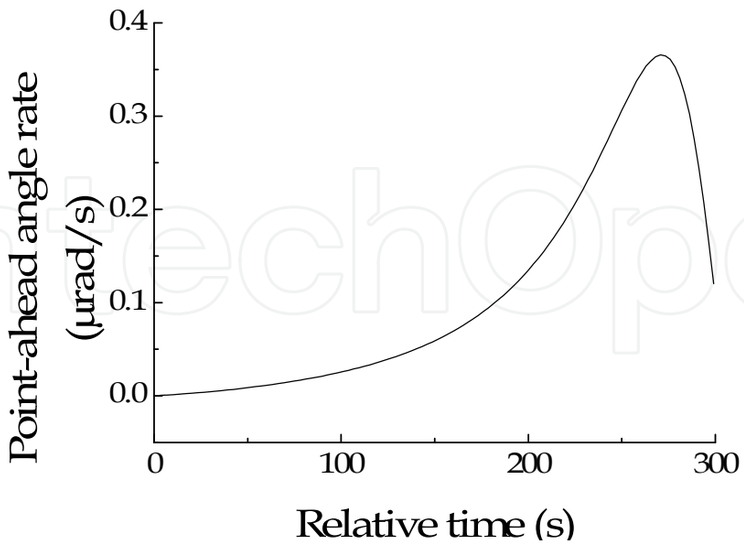

Fig. 6. Point-ahead angle rate when the maximum elevation angle at the ground station reaches 88.6 deg.

3. Trial production of actuator and its operation characteristics

We introduce the structure of the actuator prepared for the estimation of the operation characteristics. The fabricated sample is employed to the tilt mirror actuator. The mirror's reflection angle is changed with the applied voltage and is experimentally measured. With the results, we show the feasibility of the carbon nanotube actuators to be used in the laser communication equipment.

3.1 Preparation of sample

A schematic drawing of the actuator's structure is shown in the figure 7. The polymer layer is an admixture of the carbon nanotube, the ionic liquid of 1-ethyl-3-methyl-1H-imidazole-3-ium tetrafluoroboron(IV) (C6H11N2BF4) and a perfluorosulfonic acid ionomer, Nafion ® . This layer is placed between the carbon single-walled nanotube (SWNT) sheets and covered with the gold electrodes.

The figure 8(a) is a photograph of the SWNT sheets and 8(b) shows the polymer layer. The carbon nanotube is mixed with water by using ultrasonic agitation and dried to make the sheets. The fabrication of the polymer layer also uses the ultrasonic agitation to obtain the admixture paste. The paste is sandwiched between the carbon nanotube sheets and the shape is arranged.

The layered sheet covered with gold electrode is shown in the figure 9. The thickness of the gold is about 30nm. This sheet is cut to make 3 pieces actuators of the size 8mm×12mm×0.4mm. Those pieces are arranged in rotational symmetry by 120deg around the center-axis to support a mirror as shown in the figure 10. The mirror has a diameter of 20mm and is simply put on the actuators.

The actuator piece bends with applied voltage as shown in the figure 11. The bending turns in the opposite direction when the applied electrical polarity is reversed. The cross-section image of the tilt mirror is shown in the figure 12, where the notation θ is the tilt angle of the mirror and the arrows indicates the incident beam and the reflected beam.

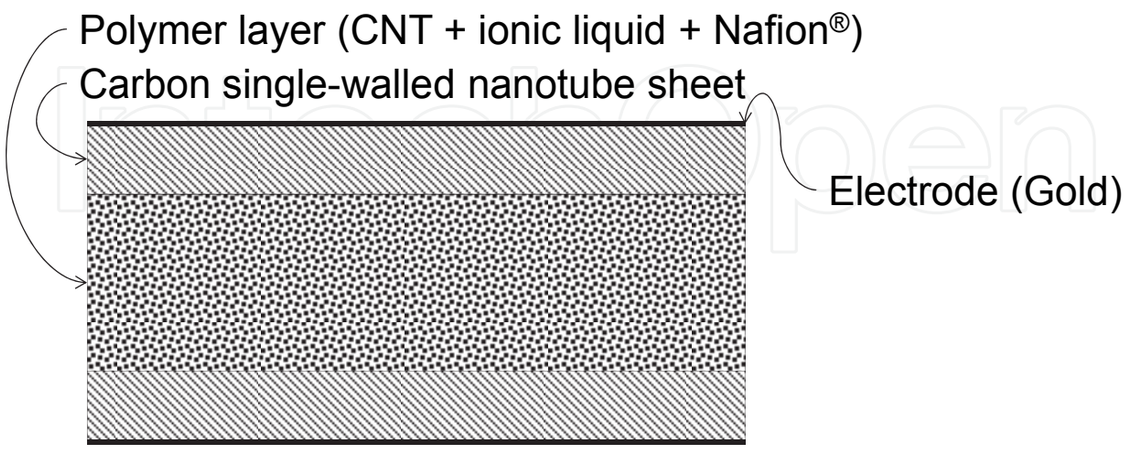

Fig. 7. Structure of the polymer actuator. Polymer layer is an admixture of CNT, ionic liquid and Nafion and is covered with CNT sheet and the gold electrode.

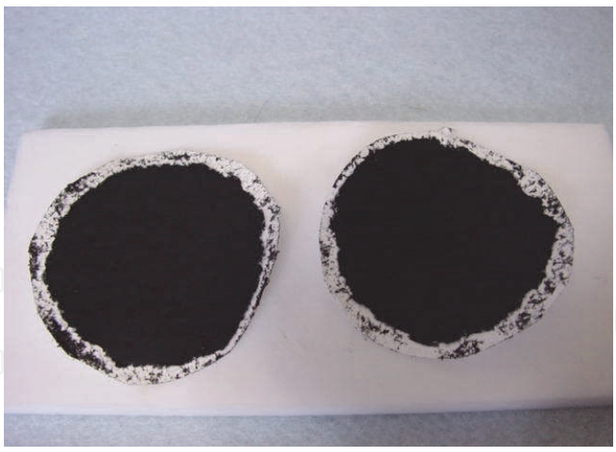

(a)

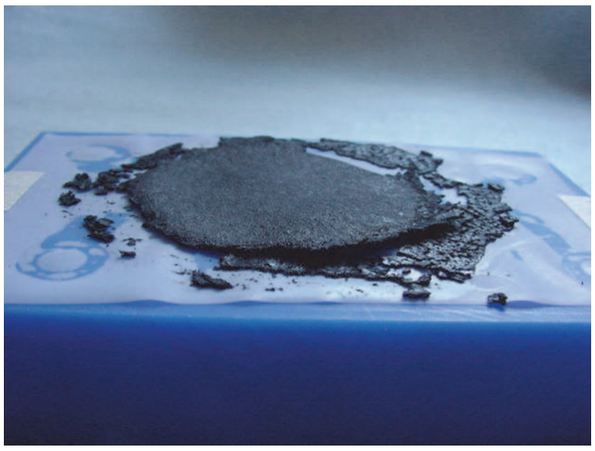

(b)

Fig. 8. (a) Carbon single-walled nanotube sheet, and (b) polymer layer with CNT, ionic liquid and Nafion® .

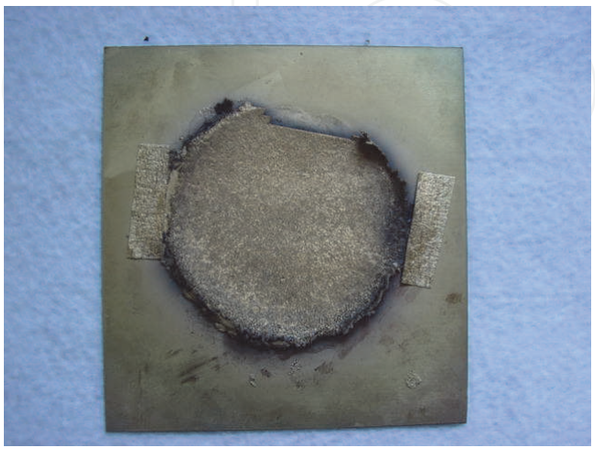

Fig. 9. Carbon nanotube sheet covered with gold.

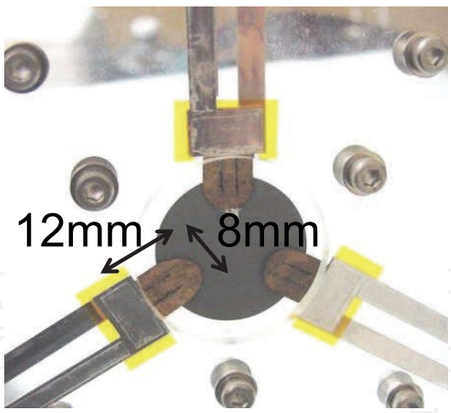

(a)

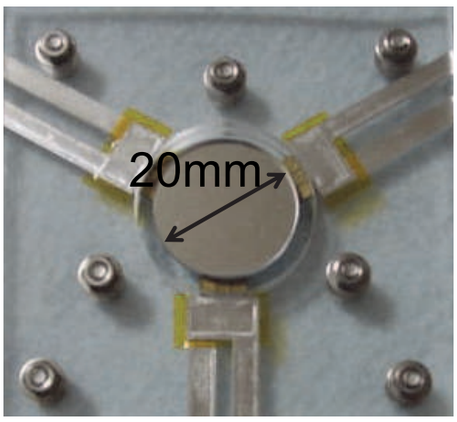

(b)

Fig. 10. Mirror supported with three carbon nanotube pieces arranged in rotational symmetry by 120deg. (a) the back side view and (b) the front side view.

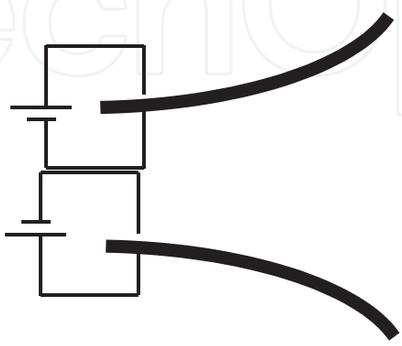

Fig. 11. Bending of actuator. The bending direction is changed with the polarity of the applied voltage.

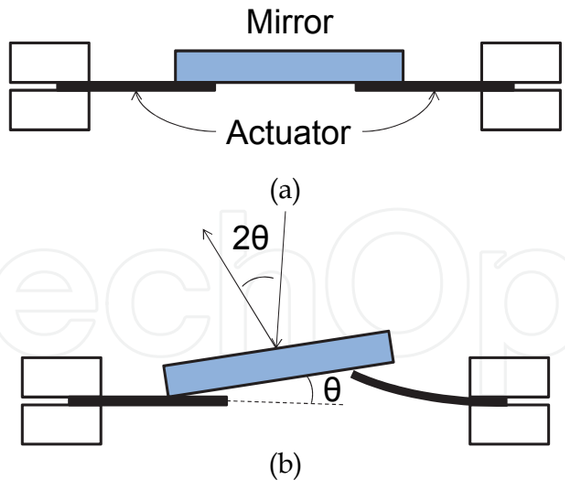

Fig. 12. (a) Cross-section of the tilt mirror, and (b) the reflection angle of light.

3.2 Operation characteristics

The bending angle of the carbon nanotube actuator depends on the applied voltage. First we carry out a long period observation of the tilt angle with the applied voltage of 2V. The measured tilt angle is shown in the figure 13, where a single actuator of the three is activated for the observation. The tilt angle is observed up to 4.4deg. Since the time taken to show such a bending angle is long, the response time should be improved much faster. But when the maximum tilt angle is only focused on, the operation range of the tilt mirror seems to cover the angular range required in the internal optics. The sample estimation for the fine pointing function in the above section indicated that the angular range to be compensated in the internal optics is within 0.1deg if the coarse pointing function steer the telescope within the accuracy of 0.01deg and the magnification factor of the internal optics is 10. That implies that even if the coarse pointing accuracy is degraded to 0.1deg, the angular range to be covered is 1.0deg and is still within the observed tilt angle.

To look at the transient characteristics around the rising period, we plot the curves in the figure 14 with the applied voltages of 1-3V, respectively. For the measurement, one of the actuators notated with the black triangle in the inset image is operated. In this figure, the circle with the solid black line bundles the plotted curves in which the tilt angles are measured along the solid arrow drawn in the inset. The circle with dashed black line means that the angles are measured along the dashed arrow direction. During the observation period, the angle variation reaches the stationary value in the case of applying 1.0V. The rising time from the 10% of the stationary value to the 90% value is estimated to 16.5 sec.

The rates of the tilt angles are calculated from the measured angles and plotted in the figure 15. The maximum rate is about 0.5mrad/s for the applied voltage of 1V, 1mrad/s for 2V and 1.25mrad/s for 3V.

To observe the transient characteristics of the back and forth motion, the voltages of +1V and -1V is applied alternately with 5s intervals. The measured results are shown in the figure 16(a). The upper image is the applied voltage and the bottom one is the measured tilt angle. According to the figure, the bending operation of the actuator seems to immediately respond to the change of the applied voltage. The peak-to-peak value ranges 1.2~1.3mrad which could be about 35% of the required angular range of ±0.1deg in the sample estimation

with the assumption of the 0.01deg accuracy for the coarse pointing and the magnification factor of 10 for the internal optics. When the voltages of ±2V are applied, the peak-to-speak value becomes about 3.3~3.6mrad as shown in the figure 16(b). This is almost the equal to the estimated angular range to be covered.
The angular rates corresponding to the figure 16(a) and 16(b) are plotted in the figure 17(a) and 17(b), respectively. According to these figures, the angular rates show almost the same transient characteristics after the several voltage alternations, which is appropriate for the fine pointing function.

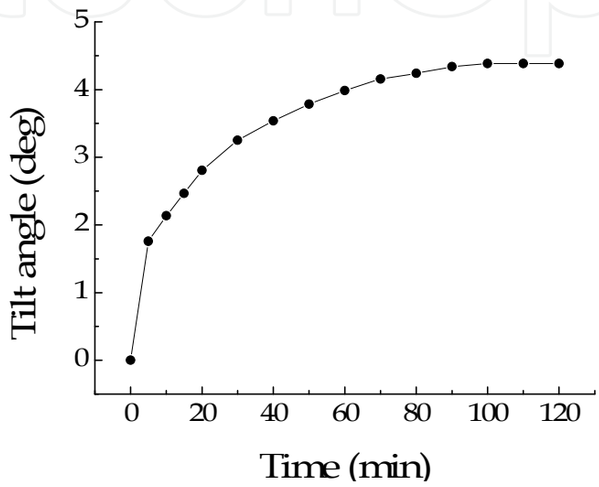

Fig. 13. A long period observation of the tilt angle of the mirror. The voltage of 2V is applied to one of the three actuators.

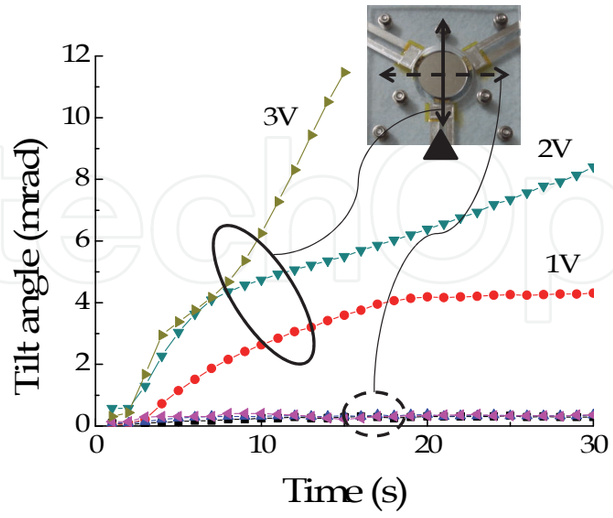

Fig. 14. Transient characteristics of the tilt angle around the rising period. The solid and dashed black circles indicate that the tilt angles are measured along the connected arrows in the inset image.

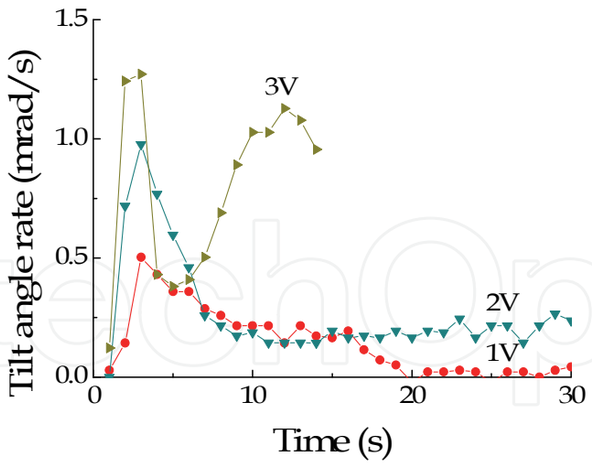

Fig. 15. Tilt angle rate around the rising period.

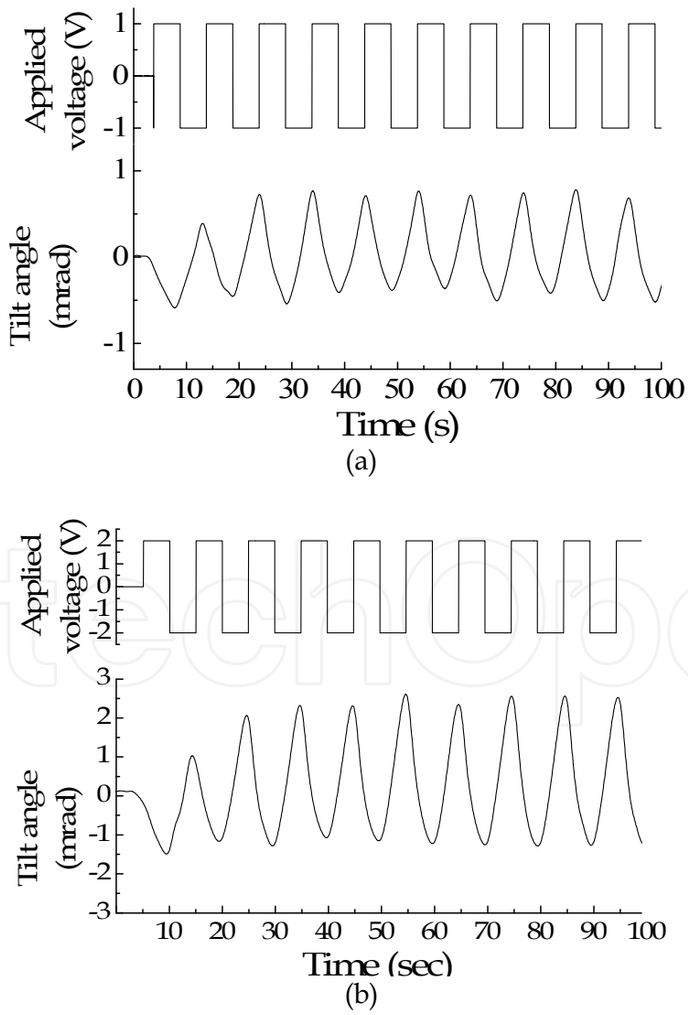

Fig. 16. Tilt angle with alternate change of applied voltage of (a) ±1V, and (b)±2V.

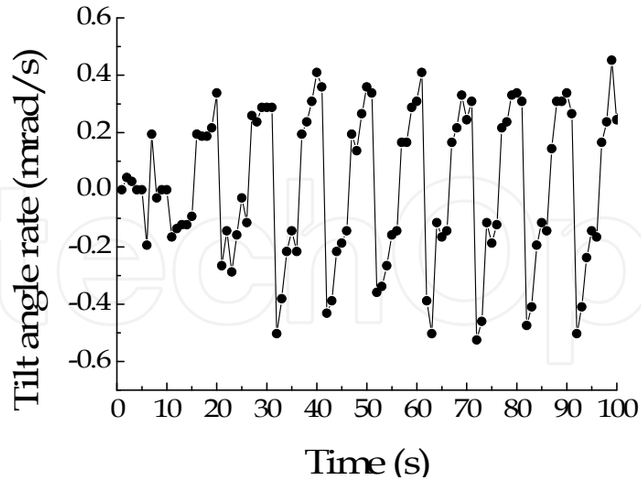

(a)

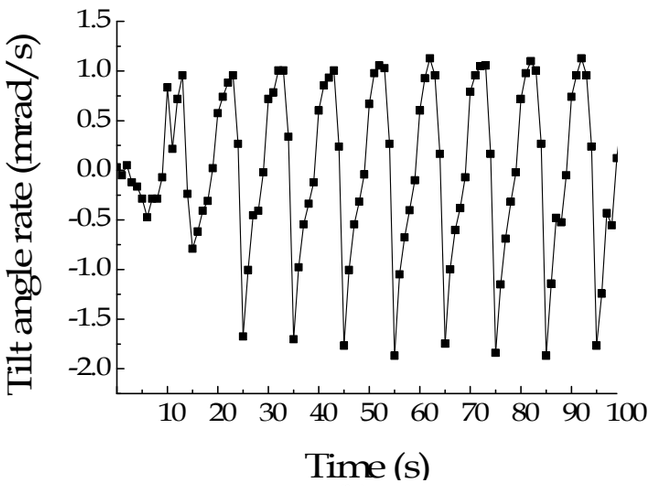

(b)

Fig. 17. Tilt angle rate with alternate change of applied voltage of (a) ±1V and (b)±2V.

4. Conclusion

In this chapter, we have carried out a feasibility study of carbon nanotube actuators as the steering functions for the optical communication terminals. We have shown a typical example of a laser communication terminal and introduced the functions of the coarse pointing, the fine pointing and the point-ahead functions as the candidates for the application of the actuators. The required characteristics for those functions are identified with the numerical analysis assuming a scenario in which a ground station tracks a satellite. We have fabricated a trial production of an actuator that is employed to make a steering function of the reflection angle of a mirror. The operation characteristics have been investigated experimentally to find the features adaptable to the laser communication equipment and the features to be improved.

Concerning the angular range, the trial production actuator should be much improved to be used in the coarse pointing function, but almost adaptable to the fine pointing and the point-ahead functions. For the angular rate, the actuator can satisfy the requirement of the point-ahead function, while the operation speed should be improved by 10times faster or more to be used in the coarse pointing function. Still the features of the carbon nanotube actuators such as the low voltage operations, light weight, simple structure, and the flexibility in the shape design are attractive for the steering functions in the optical communication terminal.

5. Acknowledgment

Taking advantage of the opportunity, we, the authors, would like to express the appreciation for the support of the Space link Co. Ltd. Tokyo Japan.

6. References

Aoki, K., Yanagita, Y., Kuroda, H. & Shiratama, K. (2004). Wide-range fine pointing mechanism for free-space laser communications, Free-Space Laser Communication and Active Laser Illumination III, Vol. 5160, pp. 495-503, ISBN 9780819450333, San Diego, CA, USA, Aug. 2003.

Bandera, P. (1999). A fine pointing mechanism for intersatellite laser communication, 8th European Space Mechanisms and Tribology Symposium, ISBN 10 9290927526, Toulouse, France, Sept. 1999.

Baughman, R. H., Cui, C., Zakhidov, A. A., Iqbal, Z., Barisci, J. N., Spinks, G. M., Wallace, G. G., Mazzoldi, A., Rossi, D. D., Rinzler, A. G., Jaschinski, O., Roth, S., Kertesz, M. (1999). Carbon nanotube actuators, Science, Vol. 284, pp. 1340-1344, ISSN 0036-8075.

Jono, T., Takayama, Y., Ohinata, K., Kura, N., Koyama, Y., Arai, K., Shiratama, K., Sodnik, Z., Bird, A. & Demelenne, B. (2006). Demonstrations of ARTEMIS-OICETS Inter-Satellite Laser Communications, 24th AIAA International Communications Satellite Systems Conference, AIAA-2006-5461, 1355, pp. 1-7, ISBN 1-56347-816-1, San Diego, CA, USA, Jun. 2006.

Jordan, G., Lyons, A. M. (2007). Thermomechanically driven polymer actuator for high-precision optical alignment, IEEE Photonics Tech. Lett., Vol. 19, pp. 212-214.

Langenbach, H., Schmid, M. (2005). Fast steering mirror for laser communication, European Space Mechanisms and Tribology Symposium, ISBN 10 9290929022, Lucerne, Switzerland, Sept. 2005.

Lu, J., Kim, S.-G., Lee, S., Oh, I.-K. (2008). Fabrication and actuation of electro-active polymer actuator based on PSMI-incorporated PVDF, Smart Mater. Struct. Vol. 17, pp. 045002-1-10.

Miller, M. J., Vucetic, B., Berry, L. (1993). Satellite Communications Mobile and Fixed Services, Kluwer Academic Publishers, Boston.

Perlot N., Knapek, M., Giggenbach, D. , Horwath, J., Brechtelsbauer M., Takayama, Y. & Jono, T. (2007). Results of the Optical Downlink Experiment KIODO from OICETS Satellite to Optical Ground Station Oberpfaffenhofen (OGS-OP), Proceedings of SPIE, Vol. 6457, pp. 645704-1-8, ISBN 9780819465733, San Jose, CA, USA, Feb. 2007.

Smutny, B., Lange, R., Kampfner, H., Dallmann, D., Muhlnikel, G., Reinhardt, M., Saucke, K., Sterr, U., Wandernoth, B. & Czichy, R. (2008). In-orbit verification of optical

inter-satellite communication links based on homodyne BPSK, Proceedings of SPIE, Vol. 6877, pp. 687702-1-6, ISBN 9780819470522, San Jose, CA, USA, Jan. 2008.

Suhonen, M., Graeffe, J., Sillanpää, T., Sipola, H., Eiden, M. (2001). Scanning micromechanical mirror for fine-pointing units of intersatellite optical links, Smart Materials and Structures, Vol. 10, pp. 1204-1210.

Tolker-Nielsen, T. & Oppenhaeuser, G. (2002). In-orbit test result of an operational optical intersatellite link between ARTEMIS and SPOT4, SILEX, *Proceedings of SPIE*, Vol. 4635, pp. 1-15, ISBN 9780819443748, San Jose, CA, USA, Jan. 2002.

Takayama, Y., Toyoshima, M., Abe, T. (2010). Low voltage actuator using carbon nanotube to tilt mirror angle, Proc. of SPIE Vol. 7587, pp. 75870K-1-6, Feb. 2010.

Toyoshima, M., Takenaka, H., Schaefer, C., Miyashita, N., Shoji, Y., Takayama, Y., Koyama, Y., Kunimori, H., Yamakawa, S. & Okamoto, E. (2009). Results from phase-4 Kirari Optical Communication Demonstration Experiments with the NICT optical ground station (KODEN), 27th AIAA International Communications Satellite Systems Conference, Vol. 13, pp. 1-9, ISBN 1-56347-941-9, Edinburgh, Scotland, Jun. 2009.

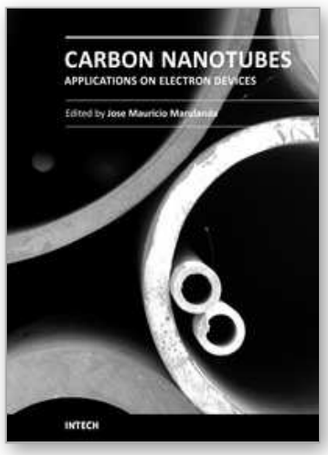

Carbon Nanotubes Applications on Electron Devices

Edited by Prof. Jose Mauricio Marulanda

ISBN 978-953-307-496-2
Hard cover, 556 pages
Publisher InTech
Published online 01, August, 2011
Published in print edition August, 2011

Carbon nanotubes (CNTs), discovered in 1991, have been a subject of intensive research for a wide range of applications. In the past decades, although carbon nanotubes have undergone massive research, considering the success of silicon, it has, nonetheless, been difficult to appreciate the potential influence of carbon nanotubes in current technology. The main objective of this book is therefore to give a wide variety of possible applications of carbon nanotubes in many industries related to electron device technology. This should allow the user to better appreciate the potential of these innovating nanometer sized materials. Readers of this book should have a good background on electron devices and semiconductor device physics as this book presents excellent results on possible device applications of carbon nanotubes. This book begins with an analysis on fabrication techniques, followed by a study on current models, and it presents a significant amount of work on different devices and applications available to current technology.

INTECH
open science | open minds

InTech Europe
University Campus STeP Ri
Slavka Krautzeka 83/A
51000 Rijeka, Croatia
Phone: +385 (51) 770 447
Fax: +385 (51) 686 166
www.intechopen.com

InTech China
Unit 405, Office Block, Hotel Equatorial Shanghai
No.65, Yan An Road (West), Shanghai, 200040, China
中国上海市延安西路65号上海国际贵都大饭店办公楼405单元
Phone: +86-21-62489820
Fax: +86-21-62489821

IntechOpen